Sensitivity of the $e^- p$ elastic cross section to the proton radius

Simone Pacetti, Egle Tomasi-Gustafsson

PANDA Collaboration Meeting
Department of Physics of Stockholm University
June 4th-8th, 2018

Agenda

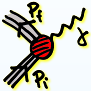

Proton radius from the scattering and atomic spectra
Formalism and data

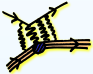

Physical limits and corrections for the scattering

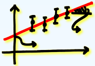

Constrained polynomial description of
proton electric form factor

Fit procedures and results

Discussion, summary and conclusions

Proton-photon vertex

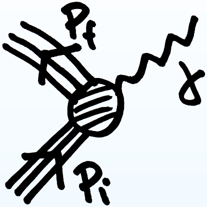

Nucleon electromagnetic four-current ($q = p_f - p_i$)

$$\langle P_f | J^{\mu}_{\mathrm{EM}}(0) | P_i \rangle = e\,\overline{u}(p_f)\left[\gamma^{\mu} F_1(q^2) + \frac{i\sigma^{\mu\nu} q_{\nu}}{2M_p} F_2(q^2)\right] u(p_i)$$

$F_1(q^2)$ and $F_2(q^2)$ are the Dirac and Pauli form factors

$F_1(0) = \mathcal{Q}_p$ $\quad$ $F_2(0) = \kappa_p$

$\mathcal{Q}_p$ = electric charge $\quad$ κ_p = anomalous magnetic moment

Breit frame

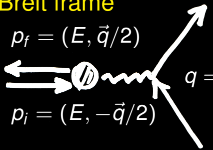

$p_f = (E, \vec{q}/2)$

$q = (0, \vec{q})$

$p_i = (E, -\vec{q}/2)$

$$\langle P_f | J^{\mu}_{\mathrm{EM}}(0) | P_i \rangle \equiv J^{\mu}_{\mathrm{EM}} = \left(J^0_{\mathrm{EM}}, \vec{J}_{\mathrm{EM}}\right)$$

$$J^0_{\mathrm{EM}} = e\left(F_1(q^2) + \frac{q^2}{4M_p^2} F_2(q^2)\right)$$

$$\vec{J}_{\mathrm{EM}} = e\,\overline{u}(p_f)\vec{\gamma}u(p_i)\left(F_1(q^2) + F_2(q^2)\right)$$

Sachs form factors

$$G_E(q^2) = F_1(q^2) + \frac{q^2}{4M_p^2} F_2(q^2)$$

$$G_M(q^2) = F_1(q^2) + F_2(q^2)$$

Normalizations

$G_E(0) = \mathcal{Q}_p$

$G_M(0) = \mu_p = \kappa_p + \mathcal{Q}_p$

μ_p = total magnetic moment

Proton radius from electron-proton scattering

In the Breit frame the Sachs form factors represent Fourier transforms of **electric charge**, $C = E$ and **magnetic moment**, $C = M$, spatial distributions.

$$G_C(q^2) = \int d^3\vec{r}\,\rho_C(\vec{r})e^{-i\vec{q}\cdot\vec{r}}$$

Assuming spherically symmetric spatial distributions, $\rho_C(\vec{r}) = \rho_C(r)$, with $r = |\vec{r}|$,

$$\widetilde{G}_C(Q^2) = \frac{4\pi}{Q}\int_0^\infty \rho_C(r)\sin(Q\,r)\,r\,dr$$

- $Q^2 = -q^2 = \vec{q}^2$ or $Q = |\vec{q}|$
- $\widetilde{G}_C(Q^2) = G_C(-Q^2)$

- Using the Taylor series of the sinus function: $\sin(x) = \sum_{k=0}^{\infty}(-1)^k \frac{x^{2k+1}}{(2k+1)!}$
- Normalizing to the total charge and magnetic moment: $\widetilde{G}_C(0) = 4\pi\int_0^\infty \rho_C(r)r^2 dr$

$$\frac{\widetilde{G}_C(Q^2)}{\widetilde{G}_C(0)} = 1 - \frac{1}{3!}\langle r^2\rangle_C Q^2 + \mathcal{O}(Q^4)$$

Mean square radius

$$\langle r^2\rangle_C = \frac{4\pi\int_0^\infty \rho_C(r)r^4 dr}{\widetilde{G}_C(0)} = -\frac{6}{\widetilde{G}_C(0)}\left.\frac{d\widetilde{G}_C(Q^2)}{dQ^2}\right|_{Q^2=0} = -6\left.\frac{d\ln\widetilde{G}_C(Q^2)}{dQ^2}\right|_{Q^2=0}$$

Atomic spectra

High-precision atomic spectroscopy can probe the composite nature of nuclei.

The finite size of the nucleus enters as a correction in the splitting between $2S_{1/2}$ and $2P_{1/2}$ levels.

$$\Delta E_n = \frac{2\pi Z\alpha}{3} |\psi_n(0)|^2 \langle r^2 \rangle$$

Electron wave function

$$|\psi_n(0)|^2 = \frac{(M_{\text{red}} Z\alpha)^3}{\pi n^3}$$

The mean square radius $\langle r^2 \rangle$ is related to the Q^2 dependence of nuclear form factor.

$$\widetilde{F}(Q^2) = 1 - \frac{\langle r^2 \rangle}{3!} Q^2 + \mathcal{O}(Q^4)$$

A Q^2-dependent form factor implies a structured nucleus.

$$\widetilde{F} = 1 \longrightarrow \widetilde{F}(Q^2) = 1 - \frac{\langle r^2 \rangle}{3!} Q^2 + \mathcal{O}(Q^4)$$

The potential acquires an additional delta-like term.

$$U(r) = -\frac{Z\alpha}{r} \longrightarrow U(r) = -\frac{Z\alpha}{r} + \frac{4\pi Z\alpha}{3!} \delta^3(r) \langle r^2 \rangle^2$$

From point-like to structured nuclei

$$J^\mu \to J^\mu \widetilde{F}^Z(Q^2)$$

Including spin effects in spin-1/2 nuclei

$$J^\mu \to J^\mu_{\rm EM} = Ze\,\overline{u}(p_f)\left[\gamma^\mu \widetilde{F}_1^Z(Q^2) + \frac{i\sigma^{\mu\nu} q_\nu}{2M_p}\widetilde{F}_2^Z(Q^2)\right] u(p_i)$$

$\widetilde{F}^Z_{1,2}(Q^2)$ are Dirac and Pauli form factors of the Z nucleus.

The $Q^2 \to 0^+$ behavior of the EM four-current gives the mean square radius

$$J^\mu_{\rm EM}(Q^2) \underset{Q^2\to 0^+}{\sim} J^\mu_{\rm EM}(0)\left[1+Q^2\left(\left.\frac{d\widetilde{F}_1^Z(Q^2)}{dQ^2}\right|_{Q^2=0} - \frac{\widetilde{F}_2^Z(0)}{4M_p^2}\right)\right] = J^\mu_{\rm EM}(0)\left(1+Q^2 \left.\frac{d\widetilde{G}_E^Z(Q^2)}{dQ^2}\right|_{Q^2=0}\right)$$

The electric mean square radius of the Z-spin-1/2 nucleus and of the **proton** in case of the **hydrogen atom** $Z=1$.

$$\langle r^2\rangle_E^Z = -6\left.\frac{d\widetilde{G}_E^Z(Q^2)}{dQ^2}\right|_{Q^2=0}$$

$$\Delta E_1 = \frac{2\alpha^4 M_{\rm red}^3}{3}\langle r^2\rangle_E$$

Reduced mass $\quad M_{\rm red} = \dfrac{M_p M_{e,\mu}}{M_p + M_{e,\mu}}$

Hydrogen and mainly muonic hydrogen spectroscopy can provide very precise measurements of the mean square radius of the **proton charge spatial distribution**.

Puzzling data on the proton radius

Science 358, 79 (2017)
From 2S-4P transition in muonic hydrogen.
Asymmetric fit function which eliminates line shifts from quantum interference of neighbouring atomic resonances.

H. Fleurbaey, Ph.D. thesis (2017)
From 1S-3S transition in atomic hydrogen.

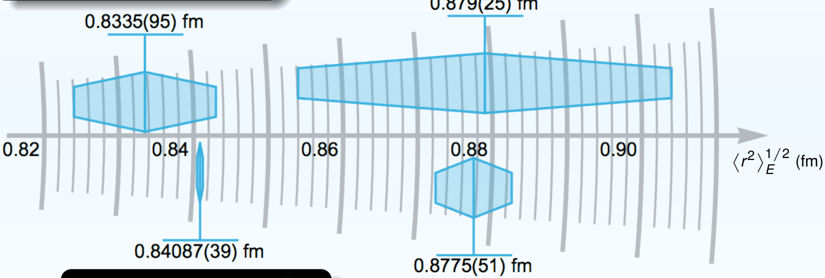

Science 339, 417 (2013)
From 2S-2P transition in muonic hydrogen.

Rev. Mod. Phys. 84, 1527 (2012)
CODATA Recommended value.
From transition in atomic hydrogen and Mainz data on electron scattering.

Strategy and formalism

We revise the possibility of extracting precise information on the proton radius from the differential cross section of the elastic electron-proton scattering

$ep \to ep$ Born cross section

$$\frac{d\sigma}{d\Omega} = \left(\frac{d\sigma}{d\Omega}\right)_{\mathrm{M}} \frac{\epsilon\, G_E^2\,(Q^2) + \tau\, G_M^2\,(Q^2)}{\epsilon\,(1+\tau)}$$

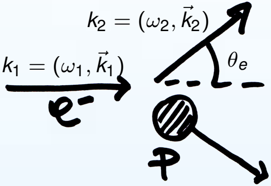

Virtual photon polarization

$$\epsilon = \frac{1}{1+2(1+\tau)\tan^2(\theta_e/2)}$$

$$\tau = \frac{Q^2}{4M_p^2}$$

Mott cross section

$$\left(\frac{d\sigma}{d\Omega}\right)_{\mathrm{M}} = \frac{4\alpha^2}{Q^4}\,\frac{\omega_2^3}{\omega_1}\left(1 - \frac{\vec{k}_1^2}{\omega_1^2}\sin^2\left(\frac{\theta_e}{2}\right)\right) \underset{M_e \ll \omega_{1,2}}{\simeq} \frac{4\alpha^2}{Q^4}\,\frac{\omega_2^3}{\omega_1}\cos^2\left(\frac{\theta_e}{2}\right)$$

- In Born approximation the differential cross section depends on two form factors $G_E(Q^2)$ and $G_M(Q^2)$ that are analytic functions of Q^2.
- In the limit $Q^2 \to 0^+$ the electric form factor $G_E(Q^2)$ is related to the mean square radius of the proton $\langle r^2 \rangle_E$.
- The extrapolation of the measured observable is needed to extract $\langle r^2 \rangle_E$.
- At low momentum transfer the differential cross section is dominated by $G_E(Q^2)$.

Physical limits

Elastic cross section diverges as $1/Q^4$ as $Q^2 = -(k_2 - k_1)^2 \to 0^+$

Mott cross section $\left(\frac{d\sigma}{d\Omega}\right)_M = \frac{4\alpha^2}{Q^4}\frac{\omega_2^3}{\omega_1}\left(1 - \frac{\vec{k}_1^2}{\omega_1^2}\sin^2\left(\frac{\theta_e}{2}\right)\right)$

- $M_e \ll \omega_{1,2} \Longrightarrow Q^2 \simeq 4\omega_1\omega_2 \sin^2(\theta_e/2)$
- $M_e^2 \gg \vec{k}_1^2 \simeq \vec{k}_2^2 \Longrightarrow Q^2 \simeq 4\vec{k}_1^2 \sin^2(\theta_e/2)$

$$\frac{d\sigma}{d\Omega} \xrightarrow[Q^2\to 0^+]{} \infty$$

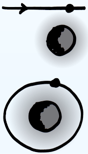

The incident electron is not deflected $\theta_e \to 0$.

Three-momenta vanish, $\vec{k}_{1,2}^2 \to 0$.
The incident electron is bounded to form a compound nucleus.

The description of the trapping process is highly model dependent.
It involves different corrections, most of which cannot be calculated exactly.

- The spin structure of the matrix elements of photo and electro-production amplitudes for the same final state are different.
- Amplitudes of photo-production reactions cannot be obtained as the static limit of electro-production amplitudes for corresponding processes.

Coulomb correction

- It is due to the multi-photon exchange between electron and proton.
- In point-like and non-relativistic limit

$$\chi(\omega_1) = \frac{\pi\alpha/\beta}{1 - e^{-\pi\alpha/\beta}}$$

$\beta = |\vec{k}_1|/\omega_1$ is the relative velocity.

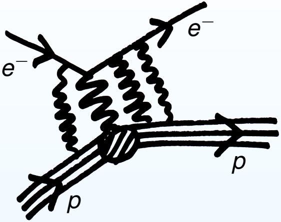

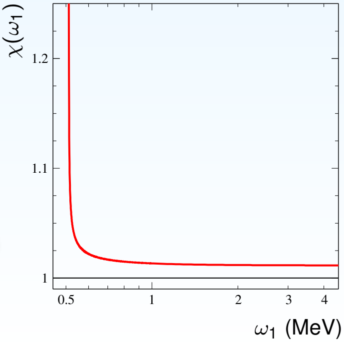

- At $\omega_1 \leq 200$ MeV, the Coulomb correction becomes greater than 1%, the same order of the error of actual cross section data.
- At $\omega_1 \leq 4$ MeV, the Coulomb correction, which is attractive for opposite charges, enhances abruptly the cross section.
- The cutoff scattering angle $\theta_{e,\mathrm{cut}} \sim 10^{-5}$, corresponding to $Q^2 \sim 10^{-5}$ MeV^2, is introduced to prevent this issue.
- At $\theta_e \leq \theta_{e,\mathrm{cut}}$ the scattering formalism is not applicable.

Lepton mass

- Neglecting lepton mass modifies the calculation of kinematic variables and cross section.
- Relative differences in the cases $M_e = 0$ and $M_e = M_e^{\mathrm{exp}}$, on Q^2 and cross section are $\leq 10^{-5}$ and $\leq 10^{-4}$ respectively at low energy.
- These effects are of the same order of the accuracy needed on the cross section measurements to discriminate between the conflicting values of the proton radius.

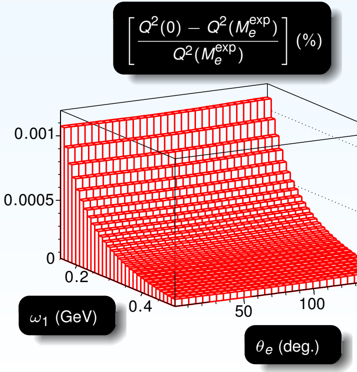

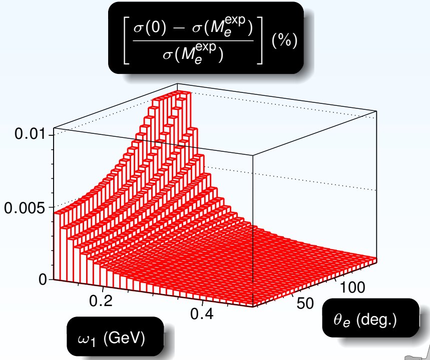

The data

Phys. Rev. Lett. **105**, 242001

We have considered only the data set of the A1 Collaboration

- It represents the most precise measurement in the largest low-Q^2 range.
- By using only one set of data, there are no normalization issues.

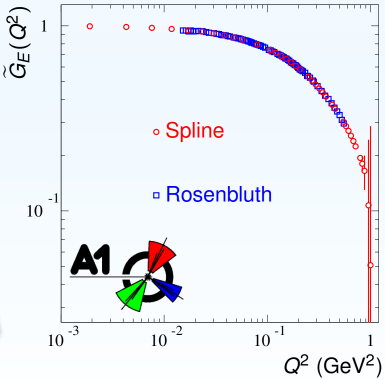

Spline - $Q^2 \geq 0.0005$ GeV^2
$\widetilde{G}_E(Q^2)$ from a global fit of the cross section based on a predefined functional form for form factors.

Rosenbluth - $Q^2 \geq 0.0152$ GeV^2
Form factors from the slope and the intercept of the reduced cross section as a function of the photon polarization ϵ at fixed Q^2.

A predefined functional form puts serious constraints on the determination of the radius

Rosenbluth data

Phys. Rev. **79**, 615

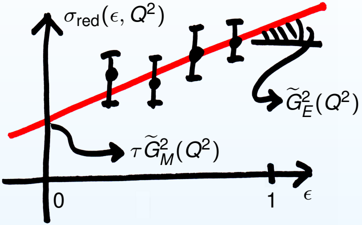

Reduced cross section $\sigma_{\rm red} = \dfrac{d\sigma/d\Omega}{(d\sigma/d\Omega)_{\rm M}}\epsilon(1+\tau)$

$$\sigma_{\rm red}(\epsilon, Q^2) = \epsilon\widetilde{G}_E^2(Q^2) + \tau\widetilde{G}_M^2(Q^2)$$

- is a function of ϵ at fixed Q^2.
- the slope gives $\widetilde{G}_E^2(Q^2)$.
- the intercept gives $\widetilde{G}_M^2(Q^2)$.

- Rosenbluth data have larger errors with respect to spline data.
- They cover a smaller Q^2 interval.
- The five points at lower Q^2 have been discarded, having been arbitrarily rescaled.

The Rosenbluth technique can be considered model independent, as it relies only on the one-photon exchange assumption.

Polynomial form factors

- $\rho_C(r) \longrightarrow$ spherically symmetric spatial distribution of a generic charge C.
- Breit frame $\longrightarrow$ no energy exchange $q^2 = (0, \vec{q})^2 = -\vec{q}^2 = Q^2$.

Form factor

$$\widetilde{G}_C(Q^2) = \frac{4\pi}{Q}\int_0^\infty \rho_C(r)\sin(Q\,r)r\,dr$$

By introducing the uniformly convergent Taylor series of the sinus function

$$\widetilde{G}_C(Q^2) = 4\pi\sum_{j=0}^\infty \frac{(-1)^n\left(Q^2\right)^n}{(2n+1)!}\int_0^\infty \rho_C(r)r^{2n+2}\,dr = G_C(0)\sum_{n=0}^\infty \frac{(-1)^n\langle r^{2n}\rangle_C}{(2n+1)!}\left(Q^2\right)^n$$

- Normalization at $Q^2 = 0$

$$\widetilde{G}_E(0) = 4\pi\int_0^\infty \rho_C(r)r^2\,dr$$

- Power-$2n$ mean radius

$$\langle r^{2n}\rangle_C \equiv \frac{1}{\widetilde{G}_E(0)}4\pi\int_0^\infty r^{2n+2}\rho_C(r)\,dr$$

- Convergence radius

$$Q^2_{RC} = \left\{\limsup_{n\to\infty}\left[\frac{\langle r^{2n}\rangle_C}{(2n+1)!}\right]^{1/n}\right\}^{-1}$$

The dipole

Standard dipole formula

$$G_D(Q^2) = \left(1 + \frac{Q^2}{0.71\ \mathrm{GeV}^2}\right)^{-2}$$

Power series

$$G_D(Q^2) = \sum_{n=0}^{\infty} \frac{(-1)^n (n+1)}{\left(0.71\ \mathrm{GeV}^2\right)^n} \left(Q^2\right)^n$$

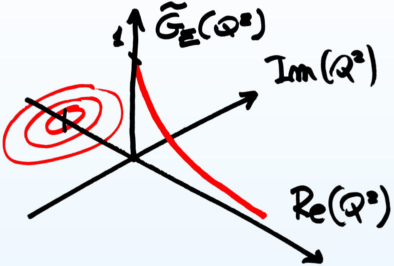

Convergence radius of the power series

$$Q^2_{RD} = \left\{ \limsup_{n\to\infty} \left[\frac{n+1}{\left(0.71\ \mathrm{GeV}^2\right)^n} \right]^{1/n} \right\}^{-1} = 0.71\ \mathrm{GeV}^2$$

Power-2n mean radii

$$\langle r^{2n} \rangle_D = \frac{(n+1)(2n+1)!}{\left(0.71\ \mathrm{GeV}^2\right)^n} = \frac{(n+1)(2n+1)!}{12^n} \langle r^2 \rangle_D^n$$

Dipole radius

$$\langle r^2 \rangle_D^{1/2} = \frac{\sqrt{12}}{\sqrt{0.71}}\, 0.1973\,\mathrm{fm} = 0.8112\,\mathrm{fm}$$

Electric form factor

$$\frac{\widetilde{G}_E(Q^2)}{G_E(0)} = 1 - \frac{1}{3!}\langle r^2\rangle_E Q^2 + \sum_{n=2}^{\infty} \frac{(-1)^n \langle r^{2n}\rangle_E}{(2n+1)!}\left(Q^2\right)^n$$

Derivative of the electric form factor

$$\frac{1}{G_E(0)}\frac{d\widetilde{G}_E}{dQ^2}(Q^2) = -\frac{1}{3!}\langle r^2\rangle_E + \sum_{n=2}^{\infty} \frac{(-1)^n \langle r^{2n}\rangle_E}{(2n+1)!} n\left(Q^2\right)^{n-1}$$

Schwarz's inequality

Given two functions $f(x), g(x) \in L^2(E)$, where $L^2(E)$ represents the set of function which are Lebesgue square integrable in $E \subset \mathbb{R} \Rightarrow$

$$\left|\int_E f^*(x)g(x)dx\right|^2 \leq \int_E |f(x)|^2\, dx \int_E |g(x)|^2\, dx$$

- $f(r) = r\sqrt{4\pi\rho(r)}r^n$
- $g(r) = r\sqrt{4\pi\rho(r)}$
- $E = (0, \infty)$

$$\left|\int_0^\infty \rho(r) r^{n+2} dr\right|^2 \leq \int_0^\infty \rho(r) r^{2n+2} dr \int_0^\infty \rho(r) r^2 dr$$

$$\langle r^n\rangle^2 \leq \langle r^{2n}\rangle \xrightarrow[\text{alegbra}]{} \langle r^2\rangle^n \leq \langle r^{2n}\rangle$$

Set of non-negative parameters with dimension of L^2

$$\mathcal{P}_N = \left\{\Delta_0^2, \langle r^2\rangle_E, \Delta_2^2, \Delta_3^2, \ldots,, \Delta_N^2\right\} \subset [0, \infty)$$

$$n \geq 2 \quad \langle r^{2n}\rangle_E = \left(\langle r^2\rangle_E + \Delta_n^2\right)^n$$

Form factor and derivative parameterizations for $N \geq 2$

- $$G_E^{\text{fit}}(Q^2; \mathcal{P}_N) = \left[1 - \frac{1}{3!}\langle r^2\rangle_E Q^2 + \sum_{n=2}^{N}(-1)^n \frac{\left(\langle r^2\rangle_E + \Delta_n^2\right)^n}{(2n+1)!}\left(Q^2\right)^n\right]\Delta_0^2$$
- $$\frac{dG_E^{\text{fit}}}{dQ^2}(Q^2; \mathcal{P}_N) = \left[-\frac{1}{3!}\langle r^2\rangle_E + \sum_{n=2}^{N}(-1)^n \frac{\left(\langle r^2\rangle_E + \Delta_n^2\right)^n}{(2n+1)!} n\left(Q^2\right)^{n-1}\right]\Delta_0^2$$

Discrete derivative

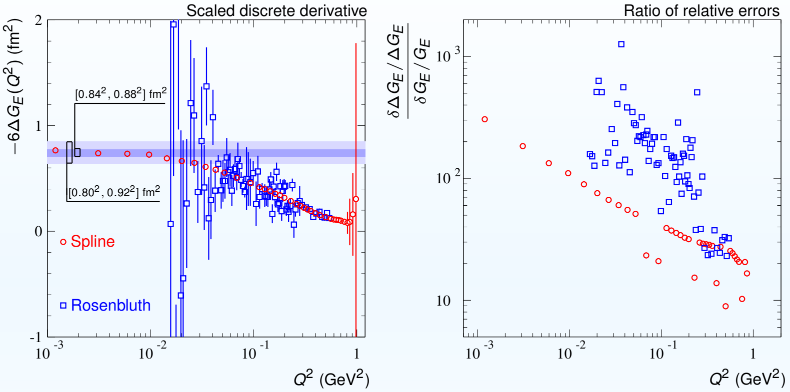

Data set on G_E

$$\left\{Q_j^2, G_{E,j}, \delta G_{E,j}\right\}$$

Discrete derivative

$$\overline{Q}_j^2 = \frac{Q_{j+1}^2 + Q_j^2}{2} \quad \Delta G_{E,j} = \frac{G_{E,j+1} - G_{E,j}}{Q_{j+1}^2 - Q_j^2} \quad \delta\Delta G_{E,j} = \frac{\sqrt{(\delta G_{E,j+1})^2 + (\delta G_{E,j})^2}}{Q_{j+1}^2 - Q_j^2}$$

A relative error of a % on the elastic cross section translates into a few % on G_E, that saturates the cross section at low Q^2, but to more than 100% on its derivative

Fitting procedure

$$\chi^2_{D,c_0,c_1,N}(Q_0^2) = c_0 \sum_{j=1}^{n_D(Q_0^2)} \left(\frac{G^D_{E,j} - G_E^{\mathrm{fit},N}\left(Q^{D2}_j\right)}{\delta G^D_{E,j}} \right)^2 + c_1 \sum_{j=1}^{n'_D(Q_0^2)} \left(\frac{\Delta G^D_{E,j} - \frac{dG_E^{\mathrm{fit},N}}{dQ^2}\left(\overline{Q^D}^2_j\right)}{\delta \Delta G^D_{E,j}} \right)^2$$

Two observables

- Function $\left\{Q^{D2}_j, G_{E,j}, \delta G_{E,j}\right\}_{j=1}^{n_D}$
- First derivative: $\left\{\overline{Q^D}^2_j, \Delta G^D_{E,j}, \delta G_{E,j}\right\}_{j=1}^{n'_D}$

Two data sets

- Rosenbluth: $D = R$
- Spline: $D = S$

10 polynomial degrees $\rightarrow$ $N = 2, 3, \ldots, 11$

Four intervals $[0, Q_0^2]$

$Q_0^2 = 0.3, 0.4, 0.5, 0.6$ GeV^2

Main data set: discrete derivative of Rosenbluth data

- The discrete derivative is the observable directly related to the radius.
- The Rosenbluth technique allows to extract FFs from differential cross section data in model-independent way.

Rosenbluth data$_{0,1}$

$\chi^2_{R,0,1,N}\left(Q_0^2\right)$

- Rosenbluth data
- Only first derivative
- All four intervals
- All ten polynomials

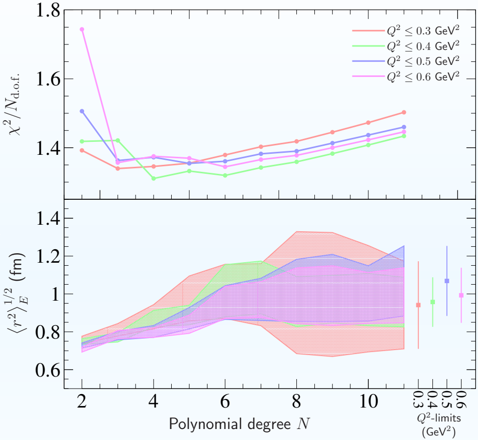

Q_0^2 (GeV^2)	0.3	0.4	0.5	0.6
$\langle r^2\rangle_E^{1/2}$ (fm)	0.94 ± 0.23	0.96 ± 0.13	1.07 ± 0.18	0.99 ± 0.15
$\frac{\chi^2_{R,0,1,11}\left(Q_0^2\right)}{N_{\mathrm{d.o.f.}}}$	1.50	1.43	1.46	1.45

Rosenbluth data$_{0,1}$

$\chi^2_{R,0,1,N}\left(Q_0^2\right)$

- Rosenbluth data
- Only first derivative
- All four intervals
- All ten polynomials

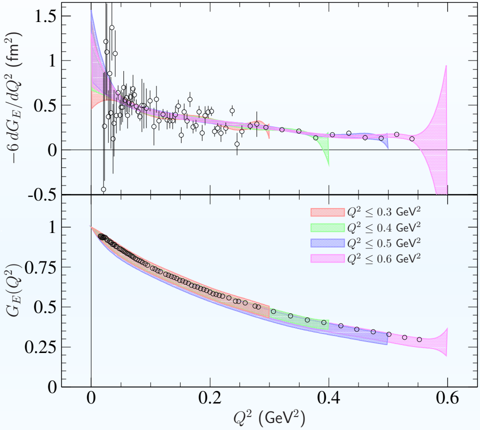

Q_0^2 (GeV^2)	0.3	0.4	0.5	0.6
$\langle r^2\rangle_E^{1/2}$ (fm)	0.94 ± 0.23	0.96 ± 0.13	1.07 ± 0.18	0.99 ± 0.15
$\frac{\chi^2_{R,0,1,11}\left(Q_0^2\right)}{N_{\text{d.o.f.}}}$	1.50	1.43	1.46	1.45

Rosenbluth $\text{data}_{1,1}$

$\chi^2_{R,1,1,N}\left(Q_0^2\right)$

- Rosenbluth data
- Function and derivative
- All four intervals
- All ten polynomials

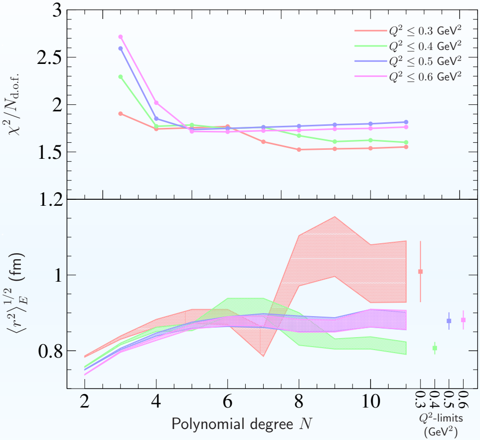

Q_0^2 (GeV^2)	0.3	0.4	0.5	0.6
$\langle r^2 \rangle_E^{1/2}$ (fm)	1.008 ± 0.081	0.807 ± 0.016	0.879 ± 0.023	0.881 ± 0.025
$\dfrac{\chi^2_{R,1,1,11}\left(Q_0^2\right)}{N_{\text{d.o.f.}}}$	1.55	1.60	1.82	1.76

Rosenbluth data$_{1,1}$

$\chi^2_{R,1,1,N}\left(Q_0^2\right)$

- Rosenbluth data
- Function and derivative
- All four intervals
- All ten polynomials

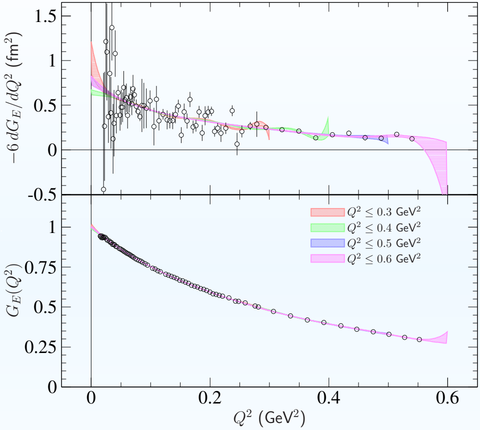

Q_0^2 (GeV^2)	0.3	0.4	0.5	0.6
$\langle r^2\rangle_E^{1/2}$ (fm)	1.008 ± 0.081	0.807 ± 0.016	0.879 ± 0.023	0.881 ± 0.025
$\frac{\chi^2_{R,1,1,11}\left(Q_0^2\right)}{N_{\mathrm{d.o.f.}}}$	1.55	1.60	1.82	1.76

Spline data$_{0,1}$

$\chi^2_{S,0,1,N}\left(Q_0^2\right)$

- Spline data
- Only first derivative
- All four intervals
- All ten polynomials

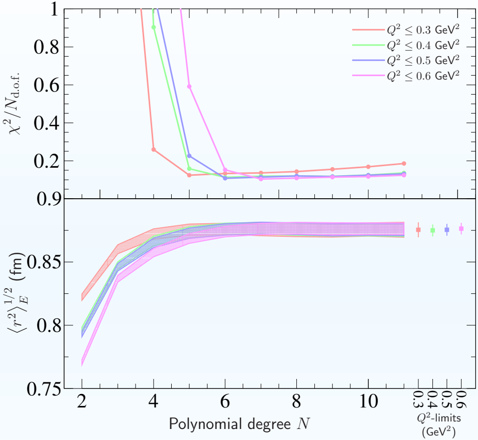

Q_0^2 (GeV^2)	0.3	0.4	0.5	0.6
$\langle r^2\rangle_E^{1/2}$ (fm)	0.875 ± 0.006	0.875 ± 0.005	0.875 ± 0.005	0.876 ± 0.005
$\frac{\chi^2_{S,0,1,11}\left(Q_0^2\right)}{N_{\mathrm{d.o.f.}}}$	0.19	0.14	0.13	0.12

Spline data$_{0,1}$

$\chi^2_{S,0,1,N}\left(Q_0^2\right)$

- Spline data
- Only first derivative
- All four intervals
- All ten polynomials

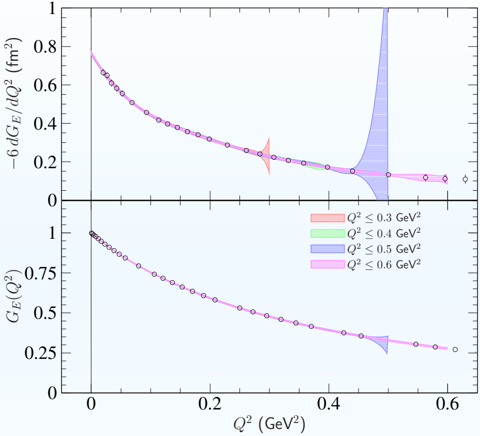

Q_0^2 (GeV^2)	0.3	0.4	0.5	0.6
$\langle r^2\rangle_E^{1/2}$ (fm)	0.875 ± 0.006	0.875 ± 0.005	0.875 ± 0.005	0.876 ± 0.005
$\frac{\chi^2_{S,0,1,11}\left(Q_0^2\right)}{N_{\mathrm{d.o.f.}}}$	0.19	0.14	0.13	0.12

Spline data$_{1,1}$

$\chi^2_{S,1,1,N}\left(Q_0^2\right)$

- Spline data
- Function and derivative
- All four intervals
- All ten polynomials

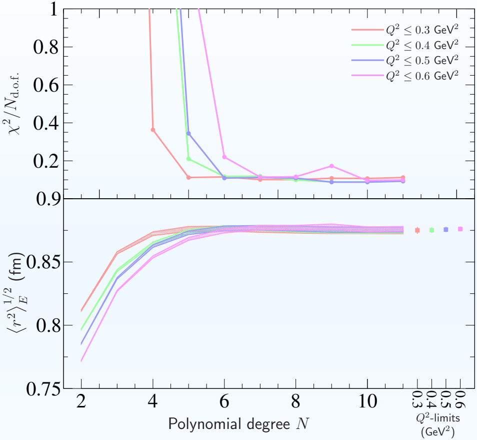

Q_0^2 (GeV^2)	0.3	0.4	0.5	0.6
$\langle r^2 \rangle_E^{1/2}$ (fm)	0.875 ± 0.003	0.875 ± 0.002	0.876 ± 0.002	0.876 ± 0.002
$\frac{\chi^2_{S,0,1,11}\left(Q_0^2\right)}{N_{\text{d.o.f.}}}$	0.11	0.09	0.09	0.10

Spline data$_{1,1}$

$\chi^2_{S,1,1,N}\left(Q_0^2\right)$

- Spline data
- Function and derivative
- All four intervals
- All ten polynomials

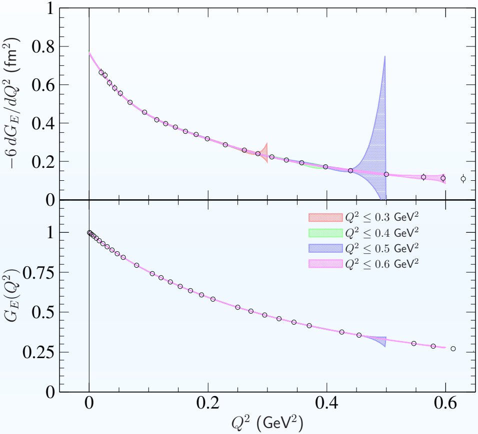

Q_0^2 (GeV^2)	0.3	0.4	0.5	0.6
$\langle r^2\rangle_E^{1/2}$ (fm)	0.875 ± 0.003	0.875 ± 0.002	0.876 ± 0.002	0.876 ± 0.002
$\frac{\chi^2_{S,0,1,11}\left(Q_0^2\right)}{N_{\mathrm{d.o.f.}}}$	0.11	0.09	0.09	0.10

Discussion

Rosenbluth only first der.	$\langle r^2\rangle_E^{1/2}$ (fm)	0.94 ± 0.23	0.96 ± 0.13	1.07 ± 0.18	0.99 ± 0.15
	$\chi^2/N_{\mathrm{d.o.f.}}$	1.50	1.43	1.46	1.45
Rosenbluth fun. + first der.	$\langle r^2\rangle_E^{1/2}$ (fm)	1.008 ± 0.081	0.807 ± 0.016	0.879 ± 0.023	0.881 ± 0.025
	$\chi^2/N_{\mathrm{d.o.f.}}$	1.55	1.60	1.82	1.76
Spline only first der.	$\langle r^2\rangle_E^{1/2}$ (fm)	0.875 ± 0.006	0.875 ± 0.005	0.875 ± 0.005	0.876 ± 0.005
	$\chi^2/N_{\mathrm{d.o.f.}}$	0.19	0.14	0.13	0.12
Spline fun. + first der.	$\langle r^2\rangle_E^{1/2}$ (fm)	0.875 ± 0.003	0.875 ± 0.002	0.876 ± 0.002	0.876 ± 0.002
	$\chi^2/N_{\mathrm{d.o.f.}}$	0.11	0.09	0.09	0.10

- The additional constraint of the function constraint reduces the error on the radius by a factor 5 - 10 for Rosenbluth data and a factor of two for spline data.

Discussion

Rosenbluth only first der.	$\langle r^2\rangle_E^{1/2}$ (fm)	0.94 ± 0.23	0.96 ± 0.13	1.07 ± 0.18	0.99 ± 0.15
	$\chi^2/N_{\mathrm{d.o.f.}}$	1.50	1.43	1.46	1.45
Rosenbluth fun. + first der.	$\langle r^2\rangle_E^{1/2}$ (fm)	1.008 ± 0.081	0.807 ± 0.016	0.879 ± 0.023	0.881 ± 0.025
	$\chi^2/N_{\mathrm{d.o.f.}}$	1.55	1.60	1.82	1.76
Spline only first der.	$\langle r^2\rangle_E^{1/2}$ (fm)	0.875 ± 0.006	0.875 ± 0.005	0.875 ± 0.005	0.876 ± 0.005
	$\chi^2/N_{\mathrm{d.o.f.}}$	0.19	0.14	0.13	0.12
Spline fun. + first der.	$\langle r^2\rangle_E^{1/2}$ (fm)	0.875 ± 0.003	0.875 ± 0.002	0.876 ± 0.002	0.876 ± 0.002
	$\chi^2/N_{\mathrm{d.o.f.}}$	0.11	0.09	0.09	0.10

- The additional constraint of the function constraint reduces the error on the radius by a factor 5 - 10 for Rosenbluth data and a factor of two for spline data.
- While spline radii are stable, Rosenbluth results depend on fitting scheme.

Discussion

Rosenbluth only first der.	$\langle r^2\rangle_E^{1/2}$ (fm)	0.94 ± 0.23	0.96 ± 0.13	1.07 ± 0.18	0.99 ± 0.15
	$\chi^2/N_{\mathrm{d.o.f.}}$	1.50	1.43	1.46	1.45
Rosenbluth fun. + first der.	$\langle r^2\rangle_E^{1/2}$ (fm)	1.008 ± 0.081	0.807 ± 0.016	0.879 ± 0.023	0.881 ± 0.025
	$\chi^2/N_{\mathrm{d.o.f.}}$	1.55	1.60	1.82	1.76
Spline only first der.	$\langle r^2\rangle_E^{1/2}$ (fm)	0.875 ± 0.006	0.875 ± 0.005	0.875 ± 0.005	0.876 ± 0.005
	$\chi^2/N_{\mathrm{d.o.f.}}$	0.19	0.14	0.13	0.12
Spline fun. + first der.	$\langle r^2\rangle_E^{1/2}$ (fm)	0.875 ± 0.003	0.875 ± 0.002	0.876 ± 0.002	0.876 ± 0.002
	$\chi^2/N_{\mathrm{d.o.f.}}$	0.11	0.09	0.09	0.10

- The additional constraint of the function constraint reduces the error on the radius by a factor 5 - 10 for Rosenbluth data and a factor of two for spline data.
- While spline radii are stable, Rosenbluth results depend on fitting scheme.
- There is discrepancy between (central) values from spline and Rosenbluth.

Discussion

Rosenbluth only first der.	$\langle r^2\rangle_E^{1/2}$ (fm)	0.94 ± 0.23	0.96 ± 0.13	1.07 ± 0.18	0.99 ± 0.15
	$\chi^2/N_{d.o.f.}$	1.50	1.43	1.46	1.45
Rosenbluth fun. + first der.	$\langle r^2\rangle_E^{1/2}$ (fm)	1.008 ± 0.081	0.807 ± 0.016	0.879 ± 0.023	0.881 ± 0.025
	$\chi^2/N_{d.o.f.}$	1.55	1.60	1.82	1.76
Spline only first der.	$\langle r^2\rangle_E^{1/2}$ (fm)	0.875 ± 0.006	0.875 ± 0.005	0.875 ± 0.005	0.876 ± 0.005
	$\chi^2/N_{d.o.f.}$	0.19	0.14	0.13	0.12
Spline fun. + first der.	$\langle r^2\rangle_E^{1/2}$ (fm)	0.875 ± 0.003	0.875 ± 0.002	0.876 ± 0.002	0.876 ± 0.002
	$\chi^2/N_{d.o.f.}$	0.11	0.09	0.09	0.10

- The additional constraint of the function constraint reduces the error on the radius by a factor 5 - 10 for Rosenbluth data and a factor of two for spline data.
- While spline radii are stable, Rosenbluth results depend on fitting scheme.
- There is discrepancy between (central) values from spline and Rosenbluth.
- The decrease of the χ^2 with the inclusion of the function constraint and the stability of the results against the different fitting procedures is a clear demonstration of the model-dependence due to the choice of spline functions.

Discussion

Rosenbluth only first der.	$\langle r^2\rangle_E^{1/2}$ (fm)	0.94±0.23	0.96±0.13	1.07±0.18	0.99±0.15
	$\chi^2/N_{d.o.f.}$	1.50	1.43	1.46	1.45
Rosenbluth fun. + first der.	$\langle r^2\rangle_E^{1/2}$ (fm)	1.008±0.081	0.807±0.016	0.879±0.023	0.881±0.025
	$\chi^2/N_{d.o.f.}$	1.55	1.60	1.82	1.76
Spline only first der.	$\langle r^2\rangle_E^{1/2}$ (fm)	0.875±0.006	0.875±0.005	0.875±0.005	0.876±0.005
	$\chi^2/N_{d.o.f.}$	0.19	0.14	0.13	0.12
Spline fun. + first der.	$\langle r^2\rangle_E^{1/2}$ (fm)	0.875±0.003	0.875±0.002	0.876±0.002	0.876±0.002
	$\chi^2/N_{d.o.f.}$	0.11	0.09	0.09	0.10

- The additional constraint of the function constraint reduces the error on the radius by a factor 5 - 10 for Rosenbluth data and a factor of two for spline data.
- While spline radii are stable, Rosenbluth results depend on fitting scheme.
- There is discrepancy between (central) values from spline and Rosenbluth.
- The decrease of the χ^2 with the inclusion of the function constraint and the stability of the results against the different fitting procedures is a clear demonstration of the model-dependence due to the choice of spline functions.

Radii obtained from the only Rosenbluth data on first derivative represent our main results

Conclusion

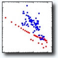

We showed that the precision on the derivative of a measured observable is lower, even by one or more orders of magnitude than that of the observable itself.

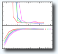

The precision can be "artificially" increased by adding physical constraints or other inputs, as a predefined functions that the (unknown) quantities should follow.

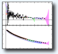

In case of an extrapolation of the derivative, pre-defined analytic functional forms do impose an even higher level of model dependence by constraining all derivatives.

Despite the loss of precision, the direct extrapolation of the Rosenbluth discrete derivative by means of first-principles-driven functional forms appears as the most reliable procedure.

The extraction of the radius, a static quantity, from a dynamical object as the cross section, is by construction affected by large systematics that cannot be reduced by the intrinsic nature of the measurement.